

NUMERICAL ANALYSIS OF AERO-SPIKE NOZZLE FOR SPIKE LENGTH OPTIMIZATION

SANOOB S N¹, PRINCE MG² & SUNDAR B³

¹Research Scholar, MES College of Engineering, Kuttipuram, Malappuram, Kerala, India

²Assistant Professor, MES College of Engineering, Kuttipuram, Malappuram, Kerala, India

³Deputy Head, VSSC, ISRO, Kerala, India

ABSTRACT

For future fully reusable SSTOs and rocket engines, light weight and high performance propulsion system from low altitude to high altitude are essential. Engines with aero spike nozzles are drawing attention as promising candidates which satisfy these requirements. A renewed interest into aerospike (plug) nozzles has surfaced for the possible replacement of standard contoured nozzles used for the propulsion systems of space vehicles. Although a more complex flow field develops on plug nozzles, the potential thrust and structural gains are attractive as the propulsive flow is free to adapt to the external stream. The commercial software Ansys-Fluent14.0 is used for the numerical simulation of the problem. Steady state analysis with implicit formulation is carried out. Mass, momentum and energy equations with k-ε turbulence model is solved.

In this project a study on various types of aero spike nozzles and characteristics of its flow field is carried out. Numerical analysis of a typical aero spike nozzle with results analysis and discussion on flow characteristics, comparison on full spike and truncated spike configuration for different pressure ratios are included. In truncated spike configuration, 20%,40%,60%,80% of spike length are included. The flow characteristics such as shock waves and wake formation etc are discussed with the help of contour plots. The performance analysis is done by plotting maximum Mach number, average exit velocity and thrust produced. Based on the analysis it can be state that the maximum performance is given by full spike nozzle. But we can provide truncation upto 60 % in order to reduce the weight and catastrophic failure due to high load on the surface.

KEYWORDS: SSTOs and Rocket Engines, NASA and Rocketdyne Research

INTRODUCTION

From the advent of rockets, launchers and space vehicles, the base principle used for the propulsion system is the classical De-Laval shaped nozzle (or alternatively simpler conical nozzles for which the following discussion also applies). This family of nozzles can be seen as a simple duct with a converging and diverging section. The flow is accelerated up to sonic speeds at the nozzle throat, it is then expanded in the diverging section because of the increased cross sectional area. These nozzles are easy to design, cheap to produce and very well mastered thus making them a good choice as primary and secondary propulsion devices. Moreover, the flow field developing in such devices is easy to predict.

However, several problems occur with such devices mainly because contoured / conical nozzles are not adaptable to the outside pressure and work optimally for one set of conditions. In space launchers, the nozzle design is made as to have optimal thrust for the trajectory part in the upper atmosphere where the ambient pressure is low and as to avoid flow separation at sea level; this is simply because most of the flight time is spent in these conditions and optimizing thrust for

high altitudes yields the highest specific impulse (ISP). The ISP is the most important criteria for a propulsion system as it directly relates to the payload that can be sent.

Flow separation at sea-level and good performance at high altitude are not compatible in terms of design and to limit this problem one uses very high pressure combustion chamber pressures. When working at off-design conditions and especially for high ambient pressures, that is for take-off and low-altitude conditions, severe problems arise.

Because of the external pressure, the flow expanding in the diverging section is pushed toward the center-line of the nozzle; this corresponds to an over-expanding jet flow. Because of this over-expansion, two phenomena appear: –first a Mach disk is created at the nozzle outlet (inducing losses and thus less thrust –then, inside the nozzle flow separation takes place. This creates high loads on the nozzle side walls and it is the source of very large vibrations which may result in catastrophic structural failures.

It can be noted that the flow separation can be asymmetric even in axisymmetric configurations and thus one must pay large attention to the flow field which becomes complex. At very high altitudes, near vacuum conditions, the jet exiting out of the contoured nozzle is pulled away from the nozzle center line, it is an under-expanding jet. Only for the design conditions, one will obtain a jet parallel to the nozzle exit walls and optimum thrust will be generated. In these operating conditions, the nozzle flow is said to be adapted.

1.1 Early Development

- NASA, the US Air Force, and Rocketdyne together works for the development of aerospike engines during the 1960-70s.
- West Germany, The propulsion arrangement consisted of a "toroidal plug nozzle" that behaved much like an aerospike with primary and secondary flows. (1965 -1970s)



Figure 1.1: First Flight with Plug Nozzle, Messerschmitt Me 262 Germany

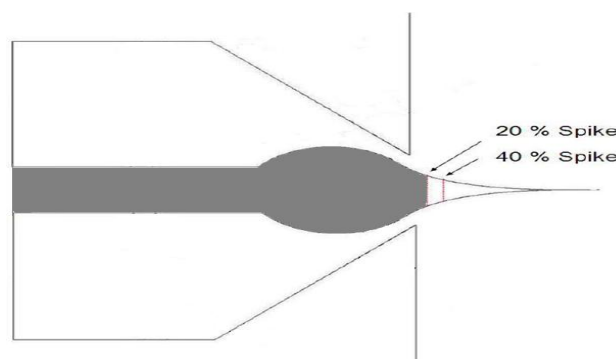


Figure 1.2: Truncated Plug Nozzle 20% and 40%

The early NASA and Rocketdyne research efforts have led to the development of the XRS-2200 linear aerospike engine that was to be used on the X-33 test vehicle. Four of these engines, subscale versions of those planned for the VentureStar vehicle, were built. Two were installed on the X-33 while the other two were being used in ground tests at the NASA Stennis Space Center in Mississippi. Each engine employed 20 combustion chambers, ten aligned on the end of each ramp centerbody, to produce 206,400 lb of thrust at sea level. The full-sized RS-2200 engine intended for the VentureStar was to have 14 combustion chambers (7 per side) to produce 431,000 lb of thrust.

1.2 Current Development

- NASA and Rocketdyne --XRS-2200 linear aerospike on the X-33 test vehicle. Each engine employed 14 combustion chambers, 7 aligned on the end of each ramp centerbody, (SSTO-RLV)
- No rocket plug nozzle of any type is believed to have actually flown until the Linear Aerospike SR-71 (BLACK BIRD) Experiment (LASRE).



Figure 1.3: Linear Aerospike SR-71 (BLACK BIRD) Experiment (LASRE)

In addition to the US test program, basic research on aerospike engines has also been undertaken in Germany, France, and Japan in recent years. The Japanese research, in particular, is quite interesting as it is intended to support the H-2A rocket and a single-stage-to-orbit (SSTO) vehicle called the HOPE-X. Unfortunately, Japan's sagging economy has caused significant cutbacks in the nation's space program and little more than concept studies and some basic experimental performance results have been generated thus far.

LITERATURE REVIEW

Aerospike nozzle is a type of nozzle with capacity of continuous altitude compensation. Aerospike nozzle is considered to have better performance at off- design altitudes compared with that of the conventional bell-shaped nozzle since its plume is open to the atmosphere outside and free to adjust, allowing the engine to operate at its optimum expansion at all altitudes.

Various experimental, analytical, and numerical research on plug nozzles have been performed since the 1950's in the Russia,[1], U.S.[2,3,13-16] Europe [4,5,6,7,8] and Japan[9]. In contrast to the previously conventional nozzle concepts, plug nozzles provide, at least theoretically, a continuous altitude adaptation up to their geometrical area ratio.

Angelino G. and Lee C. C reported two different design approaches for circular plug nozzles, which differ only in the chamber and primary nozzle layout. The designing of conical central body with more sophisticated contouring methods are also established. [10,11]

Nguyen T. V. carried out different design approaches include plug nozzles with a toroidal chamber and throat (with and without truncation) and plug nozzles with a cluster of circular bell nozzle modules or with clustered quasi rectangular nozzle modules. The latter approach seems to be advantageous because further losses induced by the gaps between individual modules and the flow field interactions downstream of the module exits can be minimized. It has been shown that transition from a round to a square nozzle results in a very small performance loss.[12]

In principle, the flow field development of a clustered plug nozzle with rectangular nozzle modules is similar to that of a toroidal plug nozzle, but avoids the inherent disadvantages of the toroidal plug design regarding

- The control of a constant throat gap during manufacturing and thermal expansion (side-loads and thrust vector deviations);
- The cooling of toroidal throat with tiny throat gaps;
- The control of combustion instabilities in the toroidal combustion chamber. Another plug nozzle configuration is the linear plug nozzle, which is foreseen for the propulsion system of the RLV X-33 concept.

Manski, D reported the details of experimental analysis carried out at DLR facility, Germany. A truncated toroidal subscale plug nozzle is used for sea-level hot-run test [3].

Hagemann G. studied performance analysis on different type of plug nozzle such as linear plug and circular, clustered plug nozzle design. The comparison of experimental results with numerical computations is also carried out. The flow field of the toroidal plug nozzle was calculated with a numerical method and reported the Mach number distribution in the combustion chamber and nozzle. Principal physical processes like expansion waves, shocks, and the recirculating base-flow region are in good agreement. Both the experiment and the numerical simulation show that the flow separates from the conical plug body before reaching its truncated end [5].

Tomita, T et. al., conducted an experimental evaluation of plug nozzle flow field and reported the parameter distribution and performance parameters with emphasizing the separation of the flow from the central plug body for conical contours. The principal flow field developments predicted by these numerical simulations are again in a good agreement with experimental data [9]. Within the frame of this ESA ARPT Program performance and flow behavior of clustered plug nozzles at different truncations are being examined by European industries and research institutes (ONERA, DLR) with subscale cold-flow plug models [7].

NUMERICAL MODELING AND ANALYSIS

3.1 Numerical Simulation

Numerical Solution for aerospike nozzle flow field is generated by using finite volume package, FLUENT. FLUENT uses control volume approach to solve fluid flow problems. In finite volume method, flow domain is discretized into called cells and analysis is done by solving the governing equations on control points on cells. The finite volume method represents and evaluates partial differential equations as algebraic equations.

The instantaneous continuity equation, momentum equation and energy equation for a compressible fluid can be written as:

Continuity Equation

$$\frac{\partial \rho}{\partial t} + \frac{\partial}{\partial x_j} [\rho u_j] = 0 \quad (3.1)$$

Momentum Equation

$$\frac{\partial}{\partial t} (\rho u_i) + \frac{\partial}{\partial x_j} [\rho u_i u_j + p \delta_{ij} - \tau_{ji}] = 0 \quad (3.2)$$

Energy Equation

$$\frac{\partial}{\partial t} (\rho e_0) + \frac{\partial}{\partial x_j} [\rho u_j e_0 + u_j p + q_j - u_i \tau_{ij}] = 0 \quad (3.3)$$

For a Newtonian fluid, assuming Stokes Law for mono-atomic gases, the viscous stress is given by

$$\tau_{ij} = 2\mu S_{ij}^* \quad (3.4)$$

Where the trace-less viscous strain-rate is defined by

$$S_{ij}^* = \frac{1}{2} \left(\frac{\partial u_i}{\partial x_j} + \frac{\partial u_j}{\partial x_i} \right) - \frac{1}{3} \frac{\partial u_k}{\partial x_k} \delta_{ij} \quad (3.5)$$

The heat-flux, q_j , is given by Fourier's law:

$$q_j = -\lambda \frac{\partial T}{\partial x_j} = -C_p \frac{\mu}{Pr} \frac{\partial T}{\partial x_j} \quad (3.6)$$

Where the laminar Prandtl number Pr is defined by:

$$Pr = \frac{C_p \mu}{\lambda} \quad (3.7)$$

To close these equations it is also necessary to specify an equation of state. Assuming a calorically perfect gas the following relations are valid:

$$\gamma = \frac{C_p}{C_v}, P = \rho RT, e = C_v T, C_v - C_p = R \quad (3.8)$$

Where γ , C_v , C_p and R are constant.

The total energy e_0 is defined by:

$$e_0 = e + \frac{U_k U_k}{2} \quad (3.9)$$

Equations (3.1)-(3.9), supplemented with gas data for γ , Pr , μ and perhaps R , form a closed set of partial differential equations, and need only be complemented with boundary conditions.

3.2 Open Turbulent Equations

In order to obtain an averaged form of the governing equations, the instantaneous continuity equation (3.1), momentum equation (3.2) and energy equation (3.3) are time-averaged. Introducing a density weighted time average decomposition (3.11) of u_i and e_0 , and a standard time average decomposition (3.10) of ρ and P gives the following exact open equations:

$$\frac{\partial \bar{\rho}}{\partial t} + \frac{\partial}{\partial x_j} (\bar{\rho} \tilde{u}_j) = 0 \quad (3.10)$$

$$\frac{\partial}{\partial t} (\bar{\rho} \tilde{u}_i) + \frac{\partial}{\partial x_j} (\bar{\rho} \tilde{u}_i \tilde{u}_j + \bar{p} \delta_{ij} + \overline{\rho u_i u_j} - \overline{\tau_{ij}}) = 0 \quad (3.11)$$

$$\frac{\partial}{\partial t}(\bar{\rho} \tilde{u}_i) + \frac{\partial}{\partial x_j}(\bar{\rho} \tilde{u}_i \tilde{u}_j + \bar{p} \delta_{ij} + \overline{\rho u_i'' u_j''} - \tau_{ij}) = 0 \quad (3.12)$$

The density averaged total energy is given by:

$$\tilde{e}_0 = \tilde{e} + \frac{\tilde{u}_k \tilde{u}_k}{2} + k \quad (3.13)$$

Where the turbulent energy, k , is defined by:

$$k = \frac{\overline{u_k'' u_k''}}{2} \quad (3.14)$$

Equation (3.10), (3.11) and (3.12) are referred to as the Favre averaged Navier-Stokes equations. $\bar{\rho}$, \tilde{u}_i and \tilde{e}_0 are the primary solution variables.

3.3 Analysis Procedure

The modeling of flow domain has been completed using geometry and mesh building software, GAMBIT. General sequence of operation involved is:

- Create full geometry and decompose into mesh able sections.
- Give meshes required.
- Continuum and boundary attachment.
- Export Mesh.

Analysis is done using FLUENT software. General sequence of operation involved is:

- Importing grid.
- Checking grid.
- Setting units.
- Define solver properties (steady, 2D/3D etc).
- Define material properties (density, viscosity variation).
- Define operating conditions.
- Define boundary conditions.
- Initialization.
- Setting convergence criteria.
- Iterating until the solution converges.

In numerical analysis various aerospace nozzle configuration is considered by varying the spike length such as 20%, 40%, 60%, 80% and 100% (full spike). Ratio of weight of spike head with full spike head for 20%, 40%, 60%, 80% and 100% truncation gives 86%, 92%, 97%, 99% and 100% simultaneously. The boundary conditions are provided in such a way that to get supersonic flow at the nozzle downstream. Different total pressure inlet conditions are analysed to get

flow behaviour at different pressure ratios. Total pressure inlet of 2 bar, 4 bar, 6 bar, 8 bar, 10 bar, 20 bar and 50 bar are considered for an outlet pressure of 1 bar.

3.4 Geometry

A schematic of the aerospike nozzle configuration [17] used is shown in Figure 3.1. The different truncated configurations are also included in the figure. The axi-symmetric model used for without truncation along with the dimensions and coordinates of contoured spike profile used is depicted in the Figure 3.2.

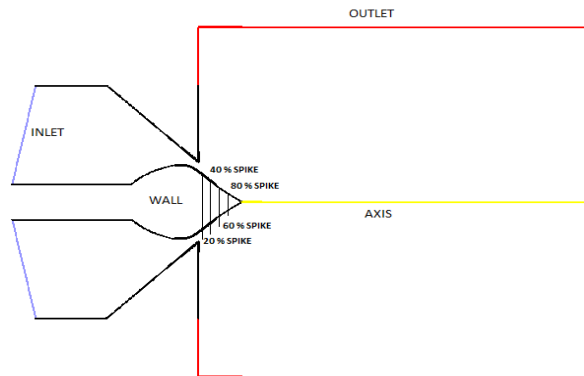
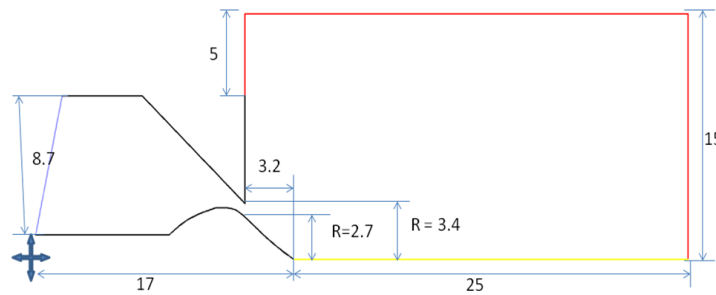


Figure 3.1: Geometry of Aerospike Nozzle Configuration



X	8.8	11.95	13.64	15.1	17
Y	1.5	3.16	2.7	1.5	0

Figure 3.2: Geometry Model Used for without Truncation

3.5 Grid System

An axi-symmetric model is used for the aerospike nozzle is used. The mesh is formed with a structured grid system having quadrilateral cells. The domain is discretised by providing more relevance on the walls, throat and nearby regions. The upstream and downstream of the domain is extended sufficiently to avoid boundary interaction on the solution. The grid system used for the analysis is shown in Figure 3.3.

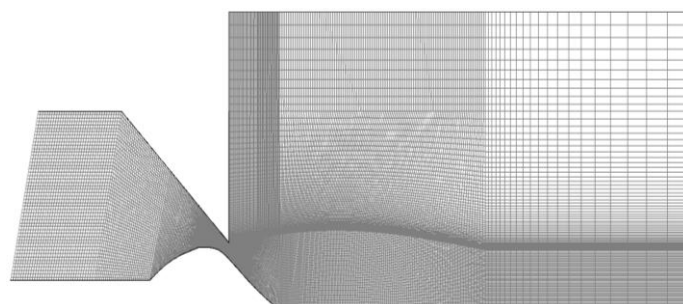


Figure 3.3: Grid System for Full Spike (100%) Nozzle

3.6 Boundary Conditions

The boundary conditions adopted are stagnation pressure and temperature at inlet of aerospike nozzle, the stagnation pressure used are 50 bar to 2 bar(for different cases). The stagnation temperatures at inlet is taken as 800K. The wall boundary is defined as Solid wall with no slip condition, pressure gradient and heat flux are set to zero. An extended domain is provided to avoid abrupt change in calculation because the property of flow at exit is not known and the flow is allowed to expand freely to atmosphere by providing the extended domain. The outlet conditions are set to that of the surrounding atmosphere. The same boundary conditions are utilized for all the cases of the present investigation.

3.7 Solver

The coupled solver, which uses a pressure based algorithm and the implicit time marching scheme are the other important solution strategies adopted in the present work. The time step required for the calculations is set as per the Courant–Friedrichs–Lewy (CFL) condition.

3.8 Grid Independence Study

The structured grid used in this study has been obtained from a systematic grid sensitivity study in which the mass flow rate, maximum exit Mach number and averaged exit velocities of different grids have been compared. The final grid used in the study has been obtained from a grid independence study done on the configuration with full spike and 10 bar total pressure inlet. The average exit velocity, maximum exit Mach number obtained and mass flow rate with different grids are compared in table 3.1.

Table 3.1: Results of Grid Independence Study

Number of Cells	Mass Flow Rate kg/s	Maximum Exit Mach Number	Average Exit Velocity m/s
14015	2.71	1.68	721.53
16818	2.74	1.7	723.8
25227	2.775	1.75	729.45
28030	2.78	1.758	730.196
33636	2.78	1.758	730.197

It can be seen that results are not different for grids with cells 28030 and 33636. Therefore the grid with number of cells equal to 28030 has been used for all the studies.

3.9 Convergence

The criterion for assessing convergence of the present steady state analysis is based on the square root of sum of squares of temporal variation of variable such as density, velocity, temperature etc.

$$RC = \left[\sum_{i=1}^N \left(\frac{\partial \zeta}{\partial t} \right)_i^2 \right]^{\frac{1}{2}} \quad (3.15)$$

Where N is the number of grid points and ζ is the variable considered. Generally, computations are stopped when residues fall below 10^{-6} .

RESULTS AND DISCUSSIONS

This chapter describes the results of numerical analysis conducted. A performance analysis has been carried out keeping the pressure inlet and the spike length as the major parameters, to optimize the geometry. Numerical analysis is done using commercial CFD software ANSYS FLUENT 14.0.

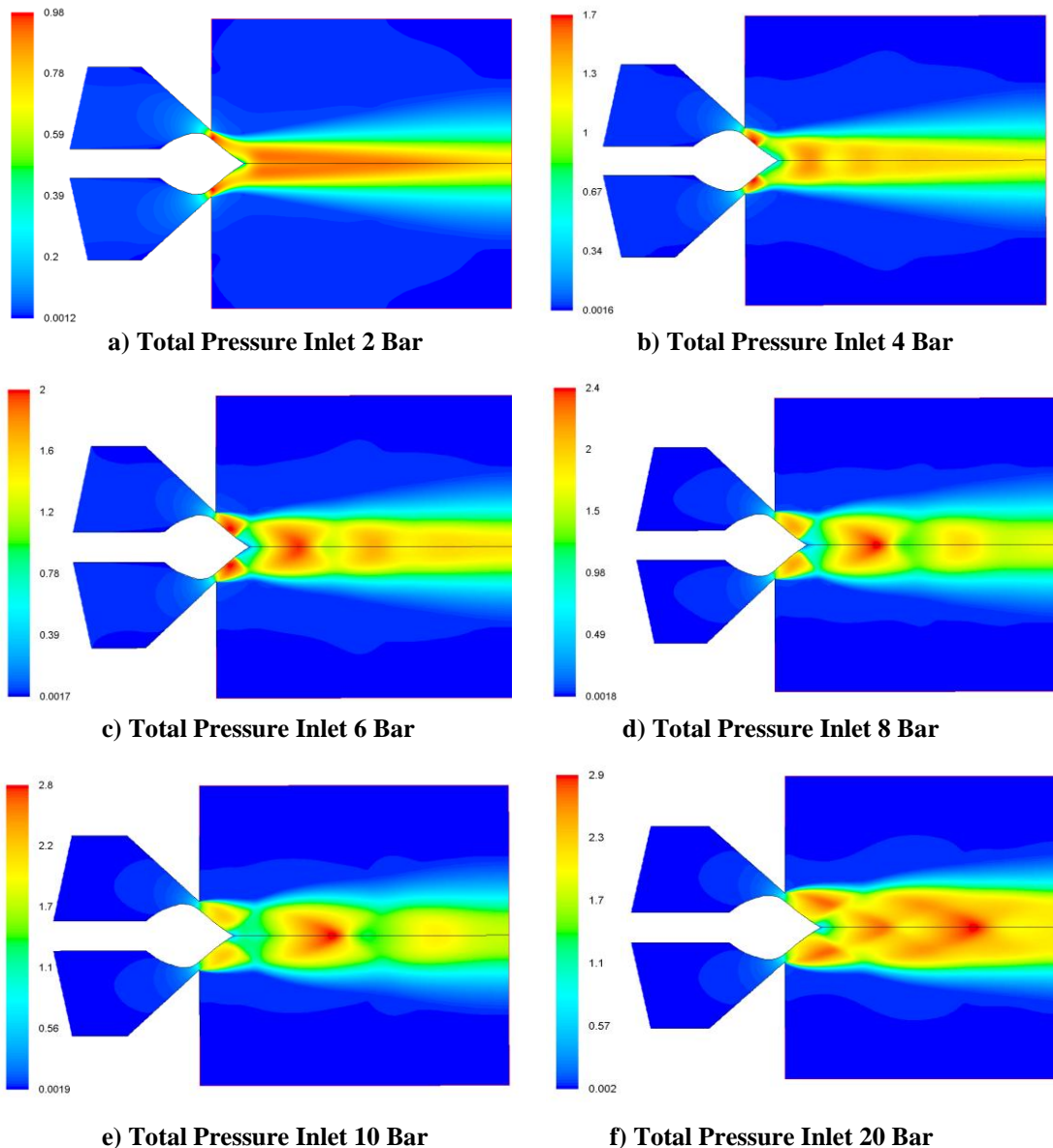
The performance of the aerospike nozzle is studied for several parameters. The flow properties such as pressure, temperature Mach number etc. are analysed and reported. The complex flow behavior inside the flow domain is identified using the counters and charts.

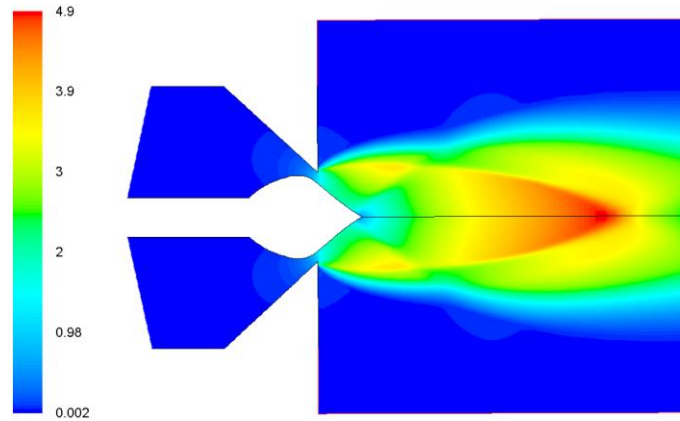
The results of the numerical analysis conducted are arranged as shown in below

- Flow through full spike nozzle: The flow behaviors in full spike nozzle for various pressure ratios are studied. The formation of shock, downstream expansion to atmosphere and thermal load at the spike surface etc. are analysed.
- Flow through truncated spike nozzle: The difference in flow behavior of truncated spike with full spike, open and closed loop formation in the base, performance comparison with full spike nozzle etc. are studied.

4.1 Flow through Full Spike Nozzle

In this section the results from the full spike (100%) configuration is included. The pressure, velocity, temperature and Mach number are depicted and discussed. The force exerted by the nozzle exit flow, interaction of shock waves, the effect of atmospheric pressure etc. and discussed.





g) Total Pressure Inlet 50 Bar

Figure 4.1: Mach Number Contours for Full Spike (100%) Nozzle

Figure 4.1 shows the contours plots of full spike nozzle configuration for different inlet boundary condition. A transition from over expanded nozzle behavior to under expanded nozzle behavior can be seen from lower pressure ratios to higher pressure ratios.

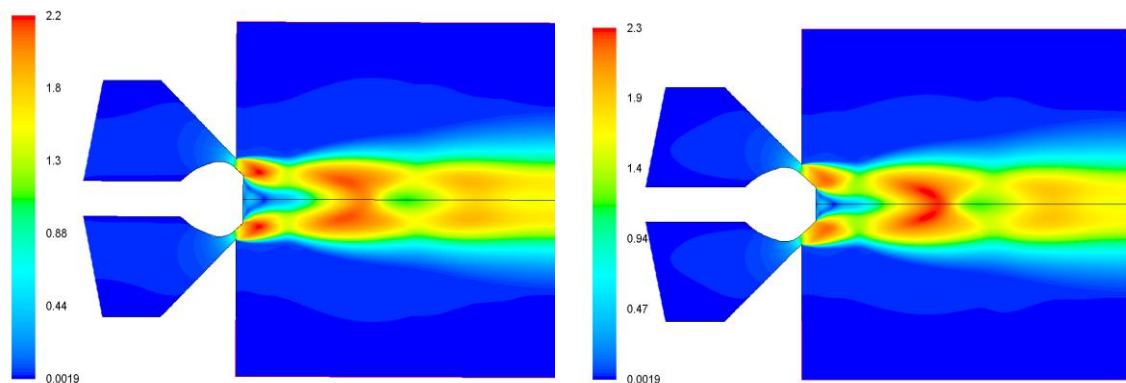
A sonic line (Mach number = 1) and shock wave interaction can be seen at the throat region for higher pressure ratios. Due to the flow behavior the outermost layer itself act like a wall boundary for the flow.

4.2 Flow through Truncated Spike Nozzle

Figure 4.2. shows the Mach number contours in different spike configurations an inlet total pressure inlet 10 bar. The figure shows a low Mach number zones near the spike bas region. As the truncation decreases the base recirculation region decreases its size and become a closed wake structure at about 60 % truncation.

At low pressure ratio exit pressure is high and greater than the nozzle static pressure at the (cowl) lip. The outer free jet boundary is close enough to the nozzle, and compression waves strike on the nozzle contour and the inner shear layer. The compression waves impinging on the nozzle contour increase the nozzle wall pressure.

The compression waves impinging on the inner shear layer surrounding the subsonic region increase the nozzle base pressure. As pressure ratio compression waves move down the nozzle contour. When ambient pressure becomes lower than the nozzle lip pressure, expansion waves form and are followed by an internal shock which no longer strike the plug contour.



a) 20 % Spike

b) 40 % Spike

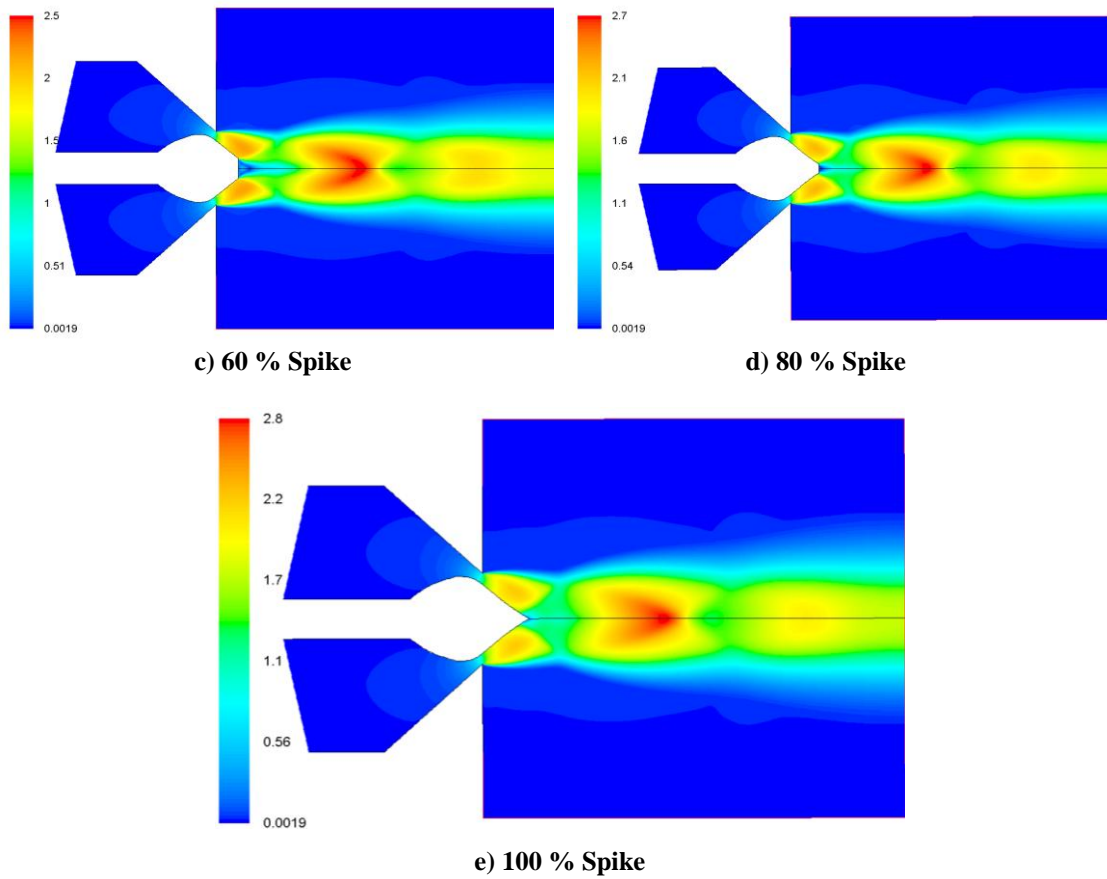


Figure 4.2: Mach Number Contours in Different Spike Configurations for a Total Pressure Inlet 10 Bar

4.3 Comparison of Performance of Different Configuration

The Figure 4.3 shows the maximum Mach number vs total pressure inlet graph. It can be seen that Mach number below 60 % truncation shows considerable changes after total inlet pressure of 6 bar. This is occurred due to the presence of long recirculation structure which will obstruct the flow even in higher pressures.

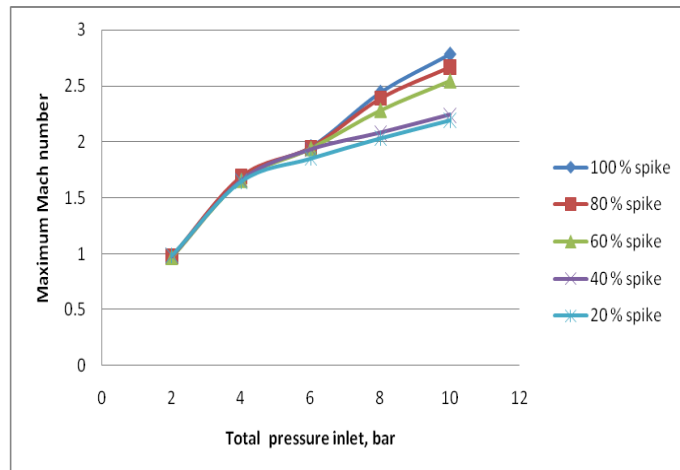


Figure 4.3: Maximum Mach Number in the Flow Domain for Various Total Pressure Inlets

The Figure 4.4 shows the average exit velocity vs total pressure inlet graph. It can be seen that average exit velocity below 60 % truncation shows considerable reduction in kinetic energy higher pressure ratios.

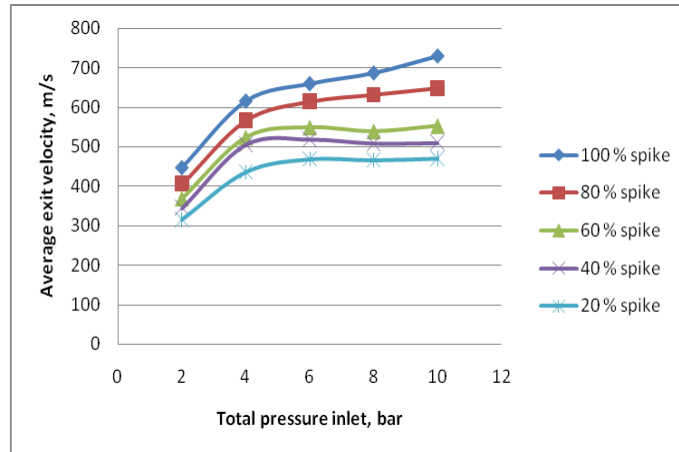


Figure 4.4: Average Exit Velocity in the Flow Domain for Various Total Pressure Inlets

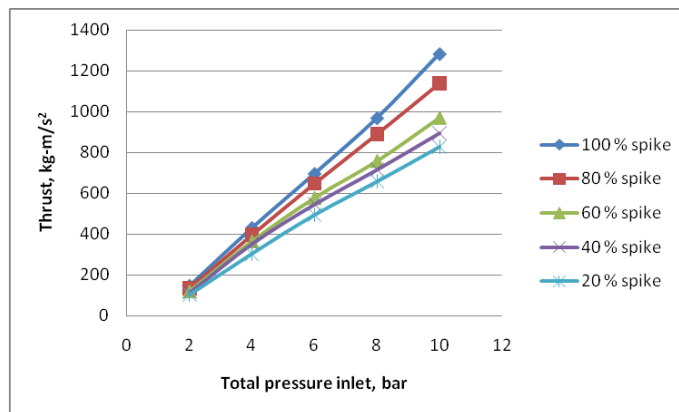


Figure 4.5: Thrust Produced for Various Total Pressure Inlets

The Figure 4.5 shows the thrust produced vs total pressure inlet graph. It can be seen that at higher pressure ratios the reduction thrust due to truncation is high compared to lower pressure ratios. The curves of 100% and 80% spike configurations gives a linear nature and from 60% onwards there is a reduction in the performance. As truncation increases the wake at spike base regions becomes large, the interaction of main flow with wake flow increases. By obstructing the main flow the sonic line at that region is shifted towards the downstream of flow and hence the reduction in performance occurs.

CONCLUSIONS

The study on aerospike nozzle is conducted with the help of available literature. Numerical analysis is carried out to identify the aerospike characteristics. Ansys-Fluent14.0 is used for the numerical simulation. Steady, implicit formulation, mass, momentum and energy conservation is carried out. The k-e turbulence model is used. The obtained flow phenomena in the aero spike flow domain are reported with the help of Mach number, static temperature, pressure and velocity plots.

The truncation effect of spike is studied by simulating configurations such as full / truncated (20%, 40%, 60% and 80%). The simulation is carried out for different pressure ratios. From the results different recirculation regions such as open and closed wake are identified. From the property distributions the causes of reduction in performance are identified as base wake behavior.

It can be observed that the maximum performance can be delivered from full spike nozzle. But truncation can be providing up to 60% in order to reduce the weight and catastrophic failure due to high load. The results indicate that up to

60% truncation gives approximately same behavior of full spike. The reduction of weight of the full spike head for 60% truncation is 3%.

REFERENCES

1. Dumnov, G. E., Nikulin, G. Z., and Ponomaryov, N. B., "Investigation of Advanced Nozzles for Rocket Engines," Space Rocket Engines and Power Plants, Vol. 4, No. 142, NIITP, 1993, pp. 10.12 –10.18.
2. Nguyen, T. V., and Pieper, J. L., "Nozzle Flow Separation," Proceedings of the 5th International Symposium of Propulsion in Space Transportation (Paris, France), 1996.
3. Manski, D., "Clustered Plug Nozzles for Future European Reusable Rocket Launchers," German Aerospace Research Establishment, 643-81/7, Lampoldshausen, Germany, 1981.
4. Immich, H., and Caporicci, M., "FESTIP Technology Developments in Liquid Rocket Propulsion for Reusable Launch Vehicles," AIAA Paper 96-3113, July 1996.
5. Hagemann, G., Schley, C.-A., Odintsov, E., and Sobatchkine, A., "Nozzle Flow field Analysis with Particular Regard to 3D-Plug-Cluster Configurations," AIAA Paper 96-2954, July 1996.
6. Immich, H., and Caporicci, M., "Status of the FESTIP Rocket Propulsion Technology Program," AIAA Paper 97-3311, July 1997.
7. "ARPT—Advanced Rocket Propulsion Technology Program, Final Reports Phase 1 and 2," European Space Agency—European Space Research and Technology Centre, The Netherlands, 1996.
8. Manolo Pires, Turbulence Modeling S And Applications To Aerospike Plug Nozzle 26TH International Congress Of The Aeronautical Sciences 2008.

